

Dual Energy Source System (Photovoltaic-Batteries) based on Three-Level Neutral Point Clamping Inverter

Farid Hadjou
Department of power Electronics
Polytechnic Military Academy
Algiers, Algeria
Hadjou_farid2020@gmail.com

Madjid Berkouk
Department of power Electronics
Polytechnic National Academy
Algiers, Algeria
emberkouk@yahoo.fr

Bekheira Tabbache
Department of power Electronics
Polytechnic Military Academy
Algiers, Algeria
laid_tabache@yahoo.com

Mohamed Benbouzid
UMR CNRS 6027 IRDL
University of Brest
Brest, France
mohamed.benbouzid@univ-brest.fr

Samir Noui
Department of power Electronics
Polytechnic Military Academy
Algiers, Algeria
nsamir05@gmail.com

Abstract—This paper deals with a dual energy source system composed of photovoltaic (PV) generator and storage elements (batteries). In this context, power converters are included to ensure the energy flow management and the permanent supply of the load. For this, a boost converter is associated to the PV generator in order to extract the maximum power, and a bidirectional DC-DC converter is connected to the element storage (batteries) to control the Direct Current (DC) bus. To ensure an alternative current supply and improve the power quality, a three-level Neutral Point Clamping (NPC) power inverter is introduced to the proposed energy system. Moreover, an inductance-capacitors (LC) filter is added also to the inverter to eliminate the high frequency harmonics. Intensive simulations are carried-out to demonstrate the effectiveness of the dual energy source system.

Keywords—Photovoltaic Generator, DC-DC Converter, NPC Inverter, MPPT

I. INTRODUCTION

Many population lives in desert and mountains areas. In general, remote areas are not connected to the electric grid due to the isolation and the installation cost. In effect, an energy source system is necessary to ensure a permanent supply. For this, diesel generators are the most means used to ensure the energies security in the remote areas. However, diesel price and transport are the main drawbacks of this solution. In hence, renewable energies present us promising solutions for remote areas. In this context, photovoltaic (PV) generators are widely used with many configurations. In literature, the most adopted system is based on PV generators and storages elements (batteries). This solution allows ensuring load supply in any time [1-2].

In this Context, this paper deals with a dual energy source system composed of photovoltaic (PV) generator and storage elements (batteries). For this, a boost converter is connected between the PV generator and DC bus to extract a maximum power from the photovoltaic source. A bidirectional DC-DC converter is added to batteries to control the common DC bus [3-4].

To ensure an alternative current supply and improve the power quality, three-level Neutral Point Clamping (NPC) power inverter is introduced to dual energy source. To

eliminate high frequency harmonics, an inductance-capacitors (LC) filter is connected to the inverter output.

To extract the maximum power from the PV generator, the DC-DC boost convert is controlled by Perturb and Observe (P&O) technique. According to the state of charge (SOC) of batteries, DC-DC reversible converter is used to regulate the DC bus of the power inverter. In other hand, the three-level NPC power inverter is supervised by Pulse Width Modulation (PWM) algorithm to ensure a fewer harmonics.

II. SYSTEM SCHEME

Figure 1 shows the dual energy source system. It composed of photovoltaic generators, batteries and power electronics converters.

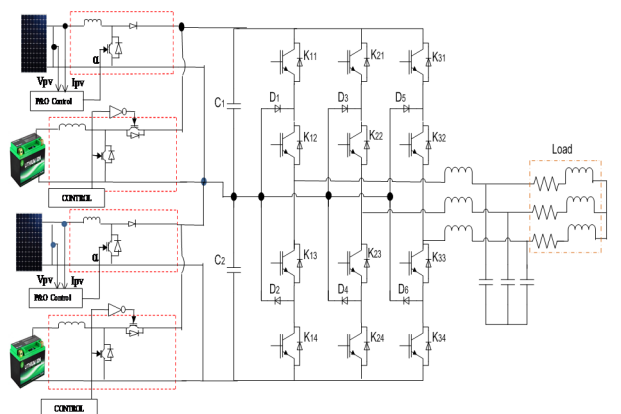


Fig.1. Dual energy source system.

The PV generators are connected to DC-DC boost converter to extract the maximum power. Another DC-DC reversible converter is associated to the batteries in order to control the common DC bus. In hence, each PV-Batteries energy system fed the upper and the lower DC bus, respectively, of the three- level NPC inverter.

A. PV generator

The photovoltaic cell, in PV generator, can be presented as an ideal current source, proportional to the incident light, in parallel with a diode. It can be modeled by Figure 2 [5-6], [7-8].

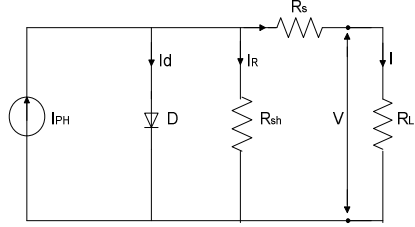


Fig.2. Equivalent electrical circuit of a PV cell

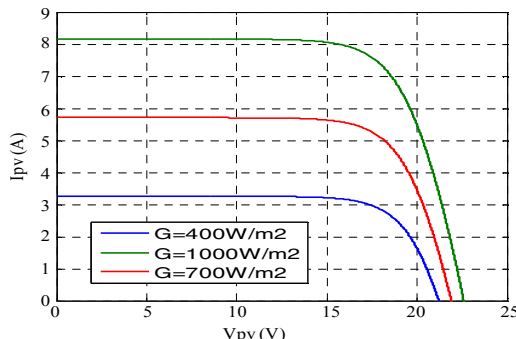
The current equation is given by:

$$I = I_{ph} - I_0 \left[\exp\left(\frac{q(V + IR_s)}{(N_{cs} \cdot \gamma \cdot k \cdot T_c)}\right) - 1 \right] - \frac{V + IR_s}{R_{sh}} \quad (1)$$

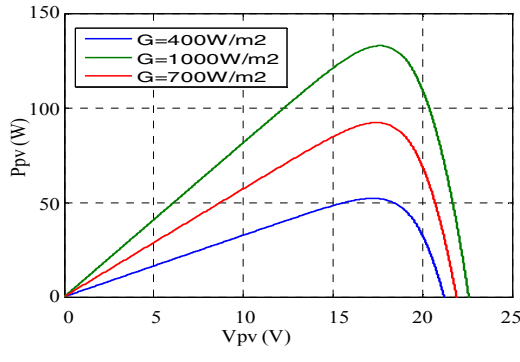
I_{ph} : photocurrent; I₀ : Diode saturation inverse current; q : coulomb constant ($1.602e-19$ C); k : Boltzman's constant ($1.38e-23$ J/K); T_c : cell temperature; γ : the quality factor of the diode, normally between 1 and 2; R_s : Series resistance; R_{sh} : shunt (or parallel) resistance [9-10].

The photocurrent I_{ph} depends to the irradiance G and the temperature T. It will be determined according to values given at reference conditions.

To obtain the desired voltage and current, a number of PV cells are interconnected together in a sealed, weather proof package called a Panel (Module) and Modules are wired in series and parallel into what is called a PV Array [11-12]. The PV generator characteristic is a non-linear with a single optimum point at maximum power.



a) The P-V curves



b) The I-V curves

Fig.3 PV array characteristics

For different irradiance values, the PV array operates with different maximum power point.

B. DC-DC Boost Converter

To extract the maximum power from PV generators, DC-DC boost converter is required. It is placed between PV generator and the DC bus. Figure 4 shows the electrical circuit of the boost converter.

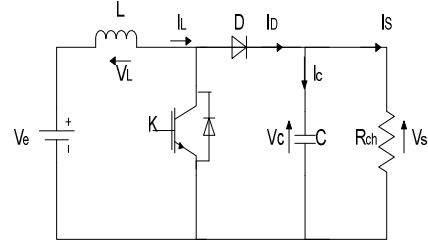


Fig.4 Boost converter Electrical circuit

For the time interval $[0 < t < \alpha T_s]$, the power switch K is ON, therefore the voltage across the diode D equal to $-V_e$, causing the diode to be reversed biased. The voltage across the inductance equals to V_e , Consequently, the magnetic energy increases.

The equations of the voltage and the current are:

$$i_c(t) = -i_s(t) \quad (2)$$

$$v_l(t) = v_e(t) \quad (3)$$

Where: T_s is the switching period; α is the duty cycle.

For the time interval $[\alpha T_s < t < T_s]$, the power switch K is turned OFF [1], the inductance acts as a current source and turns the diode ON. The equations of voltage and current are:

$$v_l(t) = v_e(t) - v_s(t) \quad (4)$$

$$i_c(t) = i_l(t) - i_s(t) \quad (5)$$

For optimal operation of the energy source system, the Maximum Power Point Tracking (MPPT) algorithm should be applied to the boost converter (Figure 5 and 6).

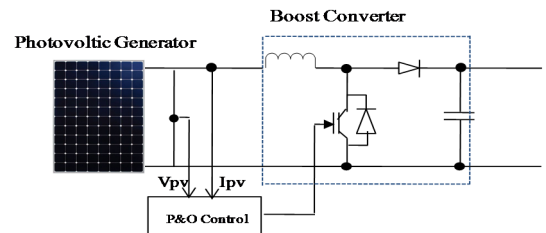


Fig.5 MPPT applied to The boot converter

The MPPT algorithm is used to perform a disturbance on the PV panel voltage by the duty cycle α . Indeed, following this disturbance, the PV panel power is calculated at each time k, and then compared with the previous one of the instant (k-1). If the power increases, the point of the maximum power is approached and the variation of the duty cycle is maintained in the same direction. Otherwise, if the power decreases, the point of the maximum power is moved. So, the direction of the variation of the duty cycle will be reversed [9-10] (Figure 6).

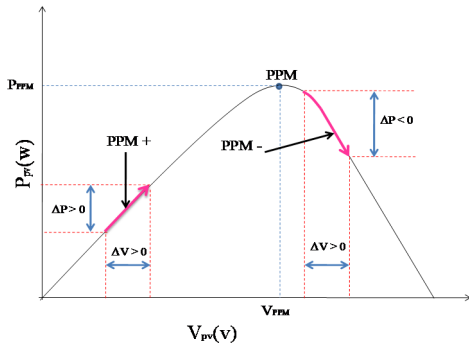


Fig.6 Perturbation and Observation scheme

C. DC-DC reversible Converter

Figure 6 illustrates the electrical circuit of the bidirectional DC-DC converter to manage the energy flow from and to the batteries.

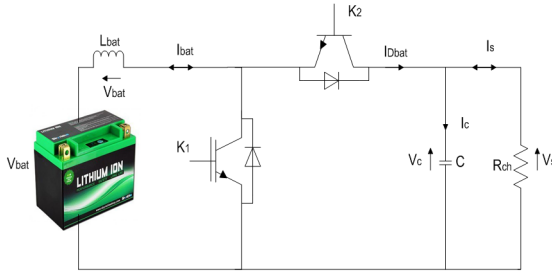


Fig.7. Bidirectional DC-DC converter

According to the direction of batteries current (I_{bat}), two configurations can be envisaged. In the first configuration, the power switch K_1 and diode D_2 operate in complementary and the batteries discharge [13-14].

From the periods time $[0 < t < \alpha_{k1} T_s]$, the equations of the voltage and the current are given by :

$$v_{Lbat}(t) = v_{bat}(t) \quad (6)$$

$$i_c(t) = -i_s(t) \quad (7)$$

For the time interval $[\alpha_{k1} T_s < t < T_s]$, the equations of the voltage and the current are given by:

$$v_{Lbat}(t) = v_{bat}(t) - v_s(t) \quad (8)$$

$$i_c(t) = -i_{Lbat}(t) - i_s(t) \quad (9)$$

In the second configuration, the power switch K_2 and diode D_1 operate in complementary and the batteries charges [4],[5].

For the time interval $[T_s < t < \alpha_{k2} T_s]$, the equations of the voltage and the current are given by

$$v_{Lbat}(t) = v_{bat}(t) - v_c(t) \quad (10)$$

$$i_c(t) = -i_{Lbat}(t) - i_s(t) \quad (11)$$

From the period $[\alpha_{k2} T_s < t < T_s]$, the equations of the voltage and the current are given by:

$$v_{Lbat}(t) = v_{bat}(t) \quad (12)$$

$$i_c(t) = +i_s(t) \quad (13)$$

The energy flow between the DC bus and the storage batteries is controlled by using the current reference in the control system of the bidirectional DC-DC converter.

These references are imposed by the control loop of the DC bus voltage (Figure 8).

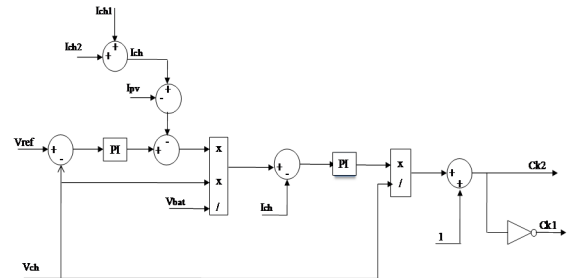


Fig. 8. DC bus control.

D. Three-level NPC Power converter

Three-level NPC inverter is used to limit the voltage stresses on power switches and improve the output voltage. Figure 9 shows the structure of a three-level NPC inverter.

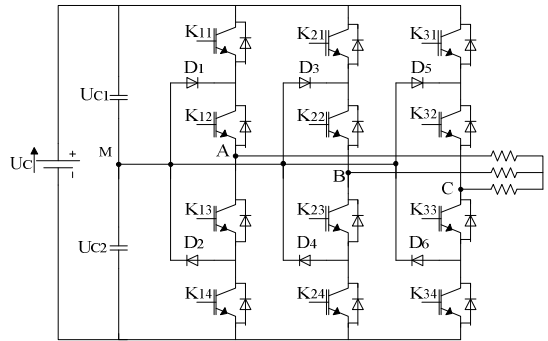


Fig.9. Three-level NPC inverter structure

Noted by F_{ki} is the connection function of the power switches. If $F_{ki}=1$, the power switch is closed. Otherwise, $F_{ki}=0$. The connection functions of the inverter are expressed by the following relations:

$$\begin{cases} F_{K1} = 1 - F_{K4} \\ F_{K2} = 1 - F_{K3} \end{cases} \quad (14)$$

With, $k = 1, 2$ or 3 , represents the leg number.

The connection function is defined as follows:

$$\begin{cases} F_{K1}^b = F_{K1} - F_{K2} \\ F_{K0}^b = F_{K3} - F_{K4} \end{cases} \quad (15)$$

Noted by: V_A , V_B and V_C are the voltages of each phase of the load. And V_{AM} , V_{BM} and V_{CM} are the midpoints voltages of each phase of the inverter. These voltages are given by the following equations:

$$\begin{cases} V_{AM} = F_{11}^b \times U_{C1} - F_{10}^b \times U_{C2} \\ V_{BM} = F_{21}^b \times U_{C1} - F_{20}^b \times U_{C2} \\ V_{CM} = F_{31}^b \times U_{C1} - F_{30}^b \times U_{C2} \end{cases} \quad (16)$$

The output voltages of the power inverter are given by:

$$\begin{bmatrix} V_A \\ V_B \\ V_C \end{bmatrix} = \frac{1}{3} \begin{bmatrix} 2 & -1 & -1 \\ -1 & 2 & -1 \\ -1 & -1 & 2 \end{bmatrix} \times \left\{ \begin{bmatrix} F_{11}^b \\ F_{21}^b \\ F_{31}^b \end{bmatrix} U_{C1} - \begin{bmatrix} F_{10}^b \\ F_{20}^b \\ F_{30}^b \end{bmatrix} U_{C2} \right\} \quad (17)$$

In term of control, Pulse Width Modulation (PWM) strategy is widely used in three-level NPC inverter. It based on the comparison between $(N-1)$ triangular signals with high frequency (fm) and amplitude (Am), and reference values of each phase with amplitude A_r and frequency f_r .

This technique is characterized by a modulation index m and a setting coefficient such as :

$$m = \frac{f_m}{f_r} \quad (18)$$

$$r = \frac{A_r}{(N-1)A_m} \quad (19)$$

The PWM algorithm principle can give us following:

$$\begin{cases} \left| V_{ref,c} \right| \leq A_m \Rightarrow T_{1,c} = 1, T_{2,c} = 0 \\ \left| V_{ref,c} \right| < A_m \text{ and } (V_{ref,c} > 0) \Rightarrow T_{1,c} = T_{2,c} = 1 \\ \left| V_{ref,c} \right| > A_m \text{ and } (V_{ref,c} < 0) \Rightarrow T_{1,c} = T_{2,c} = 0 \end{cases} \quad (20)$$

Figure 10 shows the carrier signal and the reference voltage of the first phase.

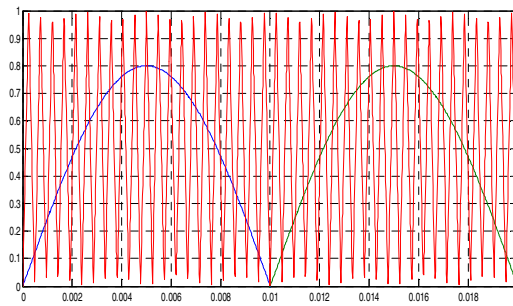


Fig.10. Reference and carrier signal

III. VALIDATION RESULTS

To check-out the developed algorithm, intensive simulations are carried out.

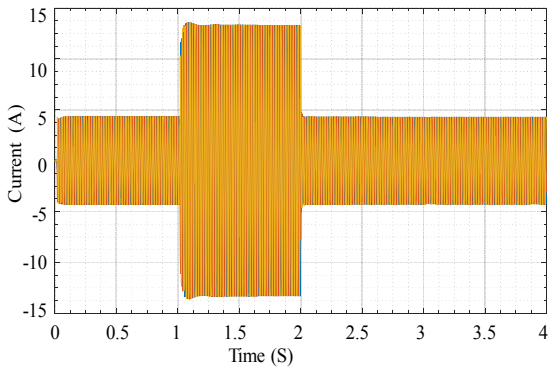


Fig 11. Lines currents

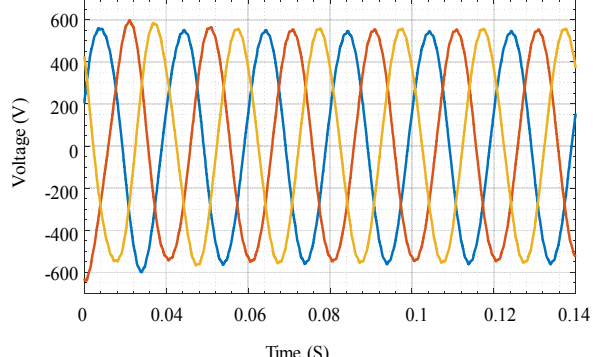
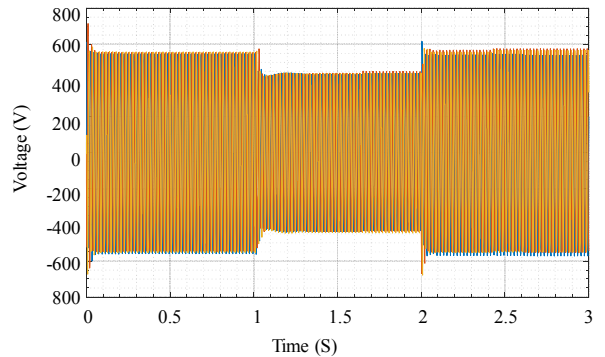


Fig 12. Load voltages

The current and the voltage provided by the three-level NPC power inverter are presented in figures 11 and 12. They have sinusoidal form with frequency of 50Hz. To improve the output inverter voltage, a passive filter is added.

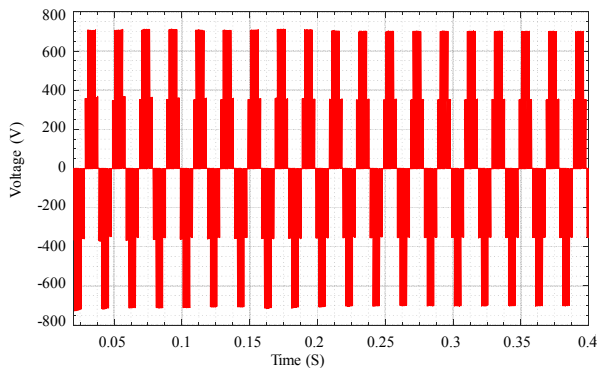


Fig13. Line to line voltage

Figure 13 illustrates the NPC inverter response in term of output voltage which three levels have been appeared. Figure 14 and 15 show the characteristics of the PV generator.

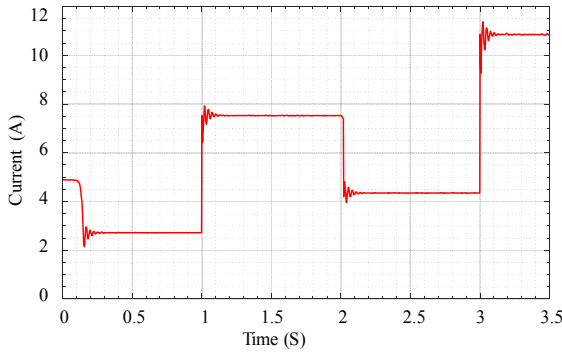


Fig.14. PV generator current

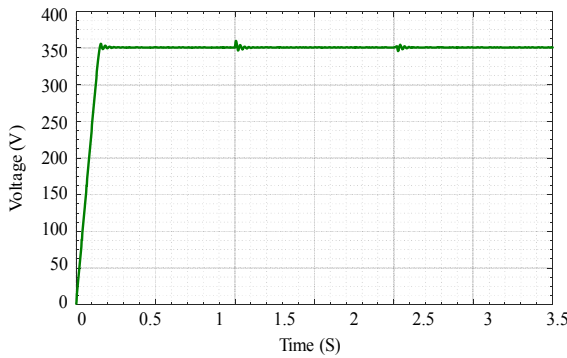


Fig.15. PV generator voltage.

The current and the voltage of the batteries are given respectively in figure 16 figure 17.

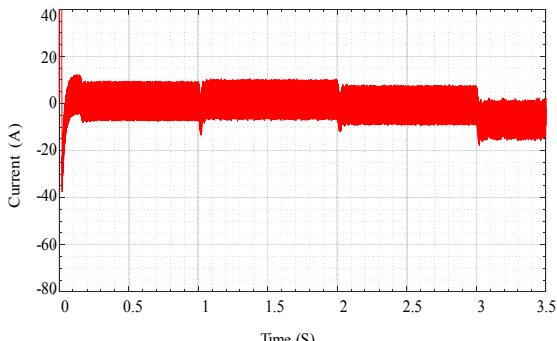


Fig.16. Batteries current

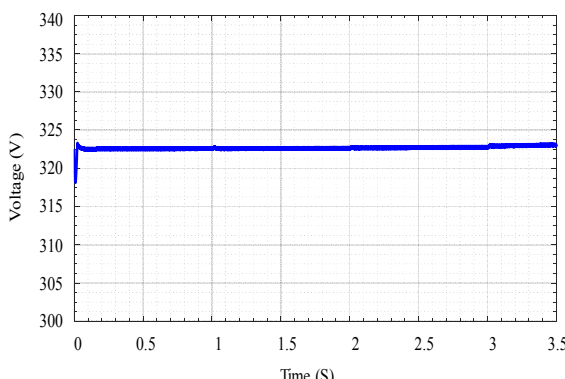


Fig.17. Batteries voltage.

Figure 18 presents the DC bus voltage of the capacitors midpoint which is maintained constant through the control loop. Figure 19 shows also the DC bus in the input of the NPC inverter. In hence, DC buses of the capacitors midpoint can be controlled by the batteries of the dual energy system.

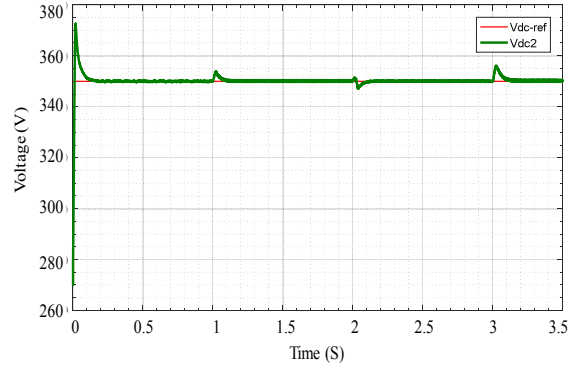


Fig. 18. DC bus of Midpoint capacitors

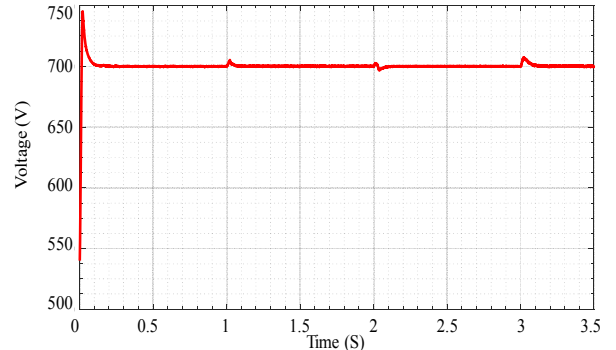


Fig.19 DC bus of the NPC inverter.

IV. CONCLUSION

This paper has presented a dual energy source system based on photovoltaic generator and storage element (batteries) for remote areas. In effect, a three level NPC Power inverter is used in order to improve the output of the proposed system. In hence, the capacitors midpoint DC bus of the NPC inverter is supplied through PV generator - batteries system. In this context, a DC-DC boost converter is placed between the PV generator and the midpoint of the DC bus to extract the maximum power from the photovoltaic source. Moreover, a bidirectional DC-DC converter is associated to the batteries in order to control the common DC bus. In addition, a passive filter (LC) is connected to the inverter output to eliminate the high frequency harmonics.

REFERENCES

- [1] M. Belouda, M. Hajjaji, H. Sliti, A. Mami, “Bi-objective optimization of a standalone hybrid PV–Wind–battery system generation in a remote area in Tunisia,” Sustainable Energy, Grids and Networks, Vol. 16, pp 315–326, December 2018.
- [2] T. Ma, M.S. Javed, “Integrated sizing of hybrid PV-wind-battery system for remote island considering the saturation of each renewable energy resource,” Energy Conversion and Management, Vol. 182, pp. 178–190, 15 February 2019.
- [3] O. A. Ahmed, J. A. M Bleijs, “An overview of DC -DC converter

topologies for fuel cell-ultracapacitor hybrid distribution system," Renewable and Sustainable Energy Reviews, Vol. 42, pp. 609-626, February 2015.

- [4] N. Zhang, D. Sutanto, K. M. Muttaqi, "A review of topologies of three-port DC-DC converters for the integration of renewable energy and energy storage system," Renewable and Sustainable Energy Reviews, Vol. 56, pp. 388-401, April 2016.
- [5] I.Guarracino, J. Freeman, A. Ramos, S.A. Kalogirou, C. N. Markides, " Systematic testing of hybrid PV-thermal (PVT) solar collectors in steady-state and dynamic outdoor conditions," Applied Energy, Vol. 240, pp.1014-1030, 15 April 2019,
- [6] M. Lämmle, A. Oliva, M. Hermann, K. Kramer, W. Kramer "PVT collector technologies in solar thermal systems: A systematic assessment of electrical and thermal yields with the novel characteristic temperature approach," Solar Energy, Volume 155, pp.867-879, October 2017.
- [7] M. Cilogullari, M. Erden, M. Karakilcik, I. Dincer, "Investigation of hydrogen production performance of a Photovoltaic and Thermal System," International Journal of Hydrogen Energy, Vol.42, Issue 4, pp 2547-2552, 26 January 2017.
- [8] R. Lamba, S. C. Kaushik, "Modeling and performance analysis of a concentrated photovoltaic-thermoelectric hybrid power generation system,"Energy Conversion and Management, Vol. 115, pp. 288-298, 1 May 2016.
- [9] H. El Achouby, M. Zaimi, A. Ibral, E. M. Assaid, "New analytical approach for modelling effects of temperature and irradiance on physical parameters of photovoltaic solar module," Energy Conversion and Management, Vol. 177, pp 258-271. 1 December 2018.
- [10] S. Shabaan, Mohamed I. Abu El-Sebah, P.Bekhit, " Maximum power point tracking for photovoltaic solar pump based on ANFIS tuning system,"Journal of Electrical Systems and Information Technology, Vol. 5, Issue 1, pp11-22. May 2018,
- [11] B. Zhao, M. Hu, X. Ao, Q. Xuan, G. Pei, "Comprehensive photonic approach for diurnal photovoltaic and nocturnal radiative cooling," Solar Energy Materials and Solar Cells, Vol. 178, pp. 266-272, May 2018,
- [12] A. Bouraiou, M. Hamouda, A. Chaker, M. Sadok, S. Lachtar, "Modeling and Simulation of Photovoltaic Module and Array Based on One and Two Diode Model Using Matlab/Simulink," Energy Procedia, Vol. 74, pp. 864-877, August 2015,
- [13] A. Abdali, R. Noroozian, K. Mazlumi, "Simultaneous control and protection schemes for DC multi microgrids systems," International Journal of Electrical Power & Energy Systems, Vol.104, pp. 230-245, January 2019.
- [14] J. Hu, Y. Shan, Y.Xu, J. M. Guerrero,"A coordinated control of hybrid ac/dc microgrids with PV-wind-battery under variable generation and load conditions," International Journal of Electrical Power & Energy Systems, Vol. 104, Pp. 583-592, January 2019.